JOURNAL OF MATERIALS SCIENCE 28 (1993) 3777–3782

Fracture study of a polyacetal resin

S. BANDYOPADHYAY
School of Materials Science and Engineering, University of New South Wales, PO Box 1, Kensington, New South Wales 2033, Australia

J. R. ROSEBLADE, R. MUSCAT
DSTO – Materials Research Laboratory, PO Box 50, Ascot Vale, Victoria 3032, Australia

Fracture experiments have been carried out with unnotched and notched tensile specimens of a polyacetal resin at room temperature at various rates of extension. An increase of approximately 13% in yield stress was observed in the unnotched tests with increased deformation rates from 1–1000 mm min^{-1}, whilst strain to failure was reduced from about 85% to approximately 0.05%. In all specimens, failure appeared to have taken place by initiation of a microscopic flaw upon yielding, and this flaw then slowly grew into a critical size when catastrophic fracture set in. In the slow-growth region, the mechanism of failure was by void growth whereby the lamellar texture was transformed into a fibrillar one. However, on the rapid fracture surface, there was evidence of lamellar texture being retained, but with small voids in the stacks of lamellae, In notched fracture specimens containing sharp razor cut, a fracture toughness, K_{Ic}, of approximately 5 MPa m$^{1/2}$ was obtained between crosshead speeds of 0.5 and 50 mm min^{-1}. At speeds of 500 and 1000 mm min^{-1}, the K_{Ic} was reduced to 4 MPa m$^{1/2}$. In the absence of a starter crack, blunt notch fracture toughness of about 6.3 MPa m$^{1/2}$ was observed at all test speeds. In specimens with a razor cut, the slow-growth region decreased as test speed increased; this can be used to construct an *R*-curve.

1. Introduction

Polyacetal resins have a useful combination of strength and stiffness (e.g. ultimate tensile strength (UTS) = 65 MPa, E = 3 GPa are common), and this makes polyacetal an attractive material for highly stressed parts, bearings, bushings and anti-friction components.

Although polyacetals are semi-crystalline polymers, their elongation to failure is much less than other semi-crystalline polymers such as nylon or polyethylene (strain to failure for polyacetal is often reported as typically 50%, compared to 400%–500% for the other materials). At room temperature, polyethylene and nylon generally exhibit necking and extensive cold drawing upon yielding, but polyacetals are normally known to fail shortly after yielding, i.e. soon after reaching the maximum load.

Studies of mechanical properties, fracture and fatigue-crack propagation of neat and toughened polyacetal resins have received considerable attention in the literature [1–6]. Chang and Yang [2] observed that at room temperature, only under very slow deformation rate (0.5 mm min^{-1} and below), polyacetals fractured in a ductile mode, and the transition deformation rate increased with increased addition of a rubbery phase used to toughen the polymer. Flexman *et al.* [6] reported that in unnotched tensile tests, neat polyacetal resins deformed principally by dilatation, whereas nylon 66 deformed mainly by shear yielding. However, in "super-tough" polyacetal, the deformation mechanism was a combination of dilatation and shear yielding. Hashemi and Williams [5] studied fracture as a function of temperature, and observed that failure of polyacetal could be divided into three categories, namely (a) brittle below approximately − 80 °C, (b) semi-brittle between − 80 and 20 °C, and (c) ductile above 20 °C.

In the present work, fracture experiments have been carried out with a polyacetal resin using (a) unnotched tensile specimens, and (b) single-edge notched specimens with and without a sharp razor starter crack at the notch tip. The experiments were conducted at room temperature, and at various rates of extension. Scanning electron microscopic (SEM) examination of fracture surfaces was undertaken for studying the microscopic aspects of deformation and fracture.

2. Materials and methods

2.1. Materials

The polymer used in this study was Delrin 107, a DuPont material which was injection moulded in the form of (a) tensile specimens approximately 10 mm wide, 4 mm thick and 60 mm gauge length (ASTM D-638 M-1), and (b) notched strips, approximately 127 mm long, 12 mm wide, 4 mm thick and a single-edge notch (SEN) of depth 2.5 mm in the middle of the length (similar to ASTM D-256 Charpy type specimens).

0022–2461

According to the manufacturer's technical specification, Delrin 107 is a polyacetal with high toughness, recommended for use as a highly stressed part, with specified tensile strength of 69 MPa, and modulus of elasticity of 3.1 GPa at room temperature. A differential scanning calorimetric study of the polymer at 10 °C min^{-1} gave a distinct melting point of approximately 173 °C and the material recrystallized well upon cooling.

2.2. Test methods

An Instron 1121 machine with a load-cell capacity of 10 kN was used to carry out the test programme. For the unnotched tensile tests, the following crosshead speeds (CHS) were employed: 1, 5, 10, 50, 100, 200, 500 and 1000 mm min^{-1} and a minimum of two specimens were tested at each CHS.

The SEN (sharp crack) specimens were tested to fracture at CHS of 0.5, 5, 10, 20, 50, 500 and 1000 mm min^{-1}, with a minimum of two specimens tested at each CHS. The sharp crack was initiated in these specimens by gently pressing a razor blade at the tip of the notch. Another set of SEN specimens, without any sharp crack, was also tested to fracture at the same CHSs; however, for this condition, only one specimen was tested at each CHS. The stress intensity factor, K, was determined by using the following calibration equation [7]

$$K = \frac{P}{BW}a^{1/2}[1.99 - 0.41\,(a/W) + 18.70\,(a/W)^2 - 38.48\,(a/W)^3 + 53.85\,(a/W)^4] \quad (1)$$

where P is the load, B the thickness, W the width, and a the crack length.

SEM studies were conducted in a Cambridge S.250 microscope after coating the fracture surfaces with gold.

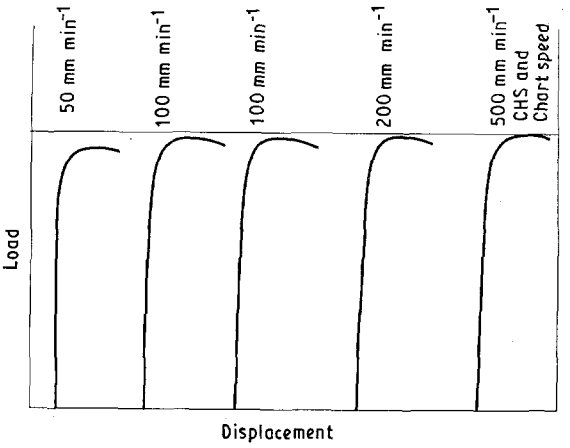

Figure 1 Representative load–displacement traces of unnotched tensile specimens showing a yield point followed by rapid failure.

TABLE I Extension to failure of the polyacetal sepcimens at various test speeds

CHS (mm min^{-1})	Approximate failure strain (%) (individual specimens)
1	58.38
	124.95
5	23.10
	24.15
10	10.29
	11.55
50	1.78
	1.78
100	0.74
	0.74
200	0.28
	0.34
500	0.06
	0.06
	0.14
	0.15
1000	0.05
	0.07
	0.09

3. Results and discussion

Representative load–displacement curves of unnotched test specimens are shown in Fig. 1, where traces are given for test speeds of 50, 100, 200 and 500 mm min^{-1}. It can be seen in Fig. 1 that (a) the specimens show a maximum load following which they fail without much further extension, and (b) the maximum load is higher for the higher speed. In Fig. 1, two traces are given for specimens tested at 100 mm min^{-1}, to illustrate the reproducibility of test results so far as the load is considered. It was also observed during the tests that extension was generally uniform, without any obvious sign of necking or cold drawing. Usually at the onset of non-linearity of the curve, the material showed evidence of stress whitening which for slow test speeds extended over a large portion of the gauge length, but was localized for the high-speed tests. The strain to failure reduced drastically with increase in test speed (Table I).

Fig. 2 gives the yield stress (taken at the maximum load) as a function of CHS for the unnotched tensile specimens, which shows that between CHS of 1 and 1000 mm min^{-1}, there is approximately 13% increase in yield stress. In general, the data points are seen to lie on a straight line, and such behaviour for semi-crystalline polymers has been attributed to activated rate-process-controlled yielding [8]. Fracture of the polyacetal specimens was mostly square, indicating that failure was predominantly plane strain. Examination of the fracture surface reveals that yielding was followed by slow growth of a microscopic sized flaw, which when reaching a critical size, led to catastrophic failure. The flaws were generally circular, sometimes elliptical, and they initiated internally, or at the surface usually at a change of section. Similar initiation and growth of internal flaws in polymers were reported by Hashemi and Williams [5].

Fig. 3 shows a low magnification view of the fracture surface of a specimen tested at CHS = 50 mm min^{-1}, which shows a circular slow-growth region in the centre of the specimen. In Fig. 4, the central part of Fig. 2 has been presented at a higher magnification. Fig. 5 shows the slow-growth region,

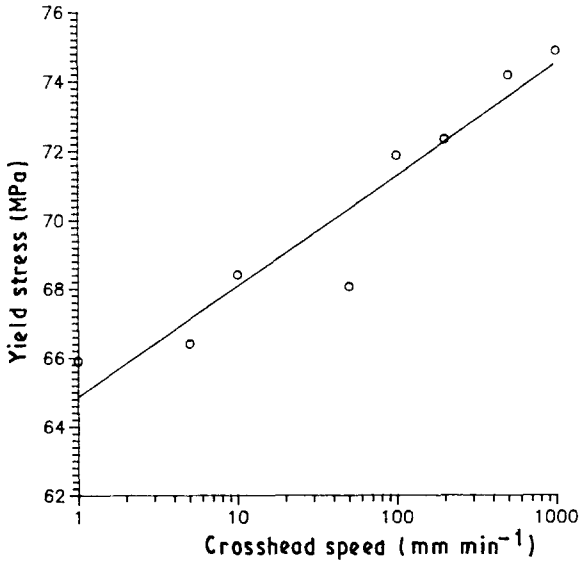

Figure 2 Yield stress versus log crosshead speed for unnotched tensile specimens.

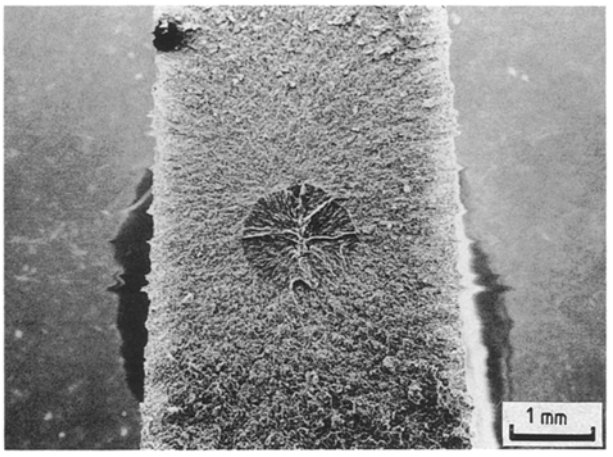

Figure 3 Low-magnification view of the fracture surface of a polyacetal unnotched tensile specimen showing initiation and growth of an internal circular flaw, and the rapid fracture area outside the flaw. Note the fracture is generally square; CHS = 50 mm min^{-1}.

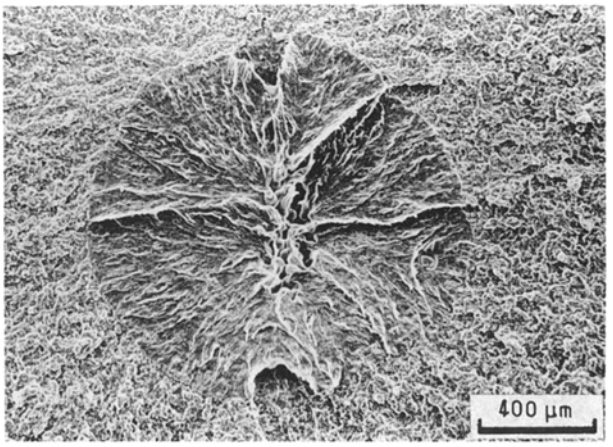

Figure 4 Higher magnification SEM view of the slow growth region of Fig. 3.

and Fig. 6 the fast-fracture region at still higher but the same magnification. It is clearly seen that the slow-growth region (Fig. 5) features with drawn fibrillar texture, that has presumably resulted from the trans-

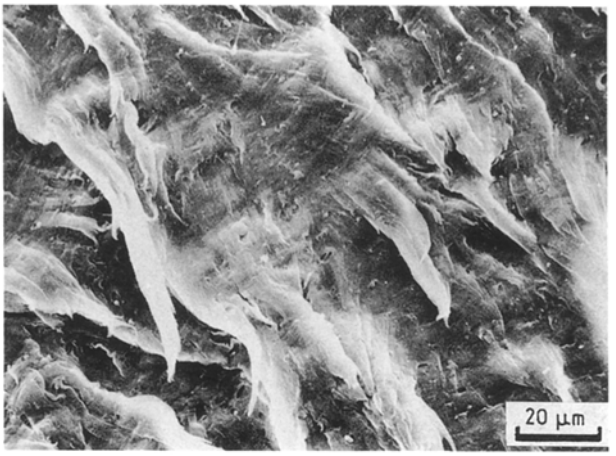

Figure 5 Much higher magnification view of fracture surface in the slow growth region showing drawn fibrillar texture.

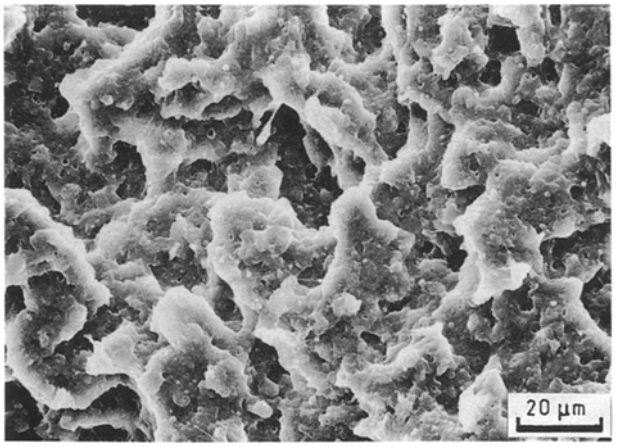

Figure 6 A totally different appearance of the fracture surface of Fig. 4 in the rapid fracture region, taken at the same magnification as Fig. 5. The features are reminiscent of spherulites that were not transformed into a fibrillar texture (see [10]).

formation of the lamellar texture, a phenomenon which has been reported for low- and high-density polyethylenes under plane strain failure at moderately slow crack speed [9, 10]. Such transformation usually occurs at comparatively higher energy level, when small voids first appear in the stacks of lamellae within the spherulites, and the voids then grow into a fibrillar texture at the expense of the lamellae. A contrasting feature is seen in the fast-fracture region (Fig. 6), showing the presence of rather undeformed spherulites, most likely as a result of interlamellar failure, as was seen in high-density polyethylene by Bandyopadhyay and Brown [10]. In fact, prolonged electron radiation at a still higher magnification (Fig. 7) confirms the presence of lamellar texture in this part of the fracture surface, albeit there are a number of small voids in the lamellae. Clearly, the speed of fast fracture did not allow transformation of the lamellar texture into a fibrillar one. It may be of interest to note that trans-spherulitic failure [4, 7] and also secondary cracking along spherulite boundaries [4] have been suggested as modes of crack propagation in fatigue studies of polyacetal [4, 11].

The results of notched fracture tests are given in Table II, where fracture toughness data for specimens

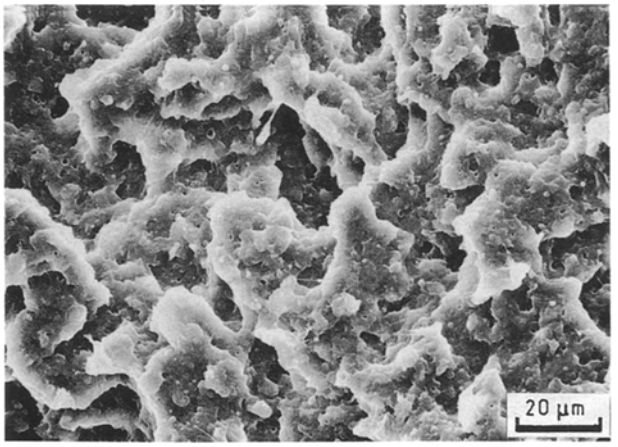

Figure 7 Higher magnification view of Fig. 6 after prolonged electron irradiation in the SEM, highlighting the lamellar texture of the sperulites, with a number of small holes initiated in the lamellar stacks.

with sharp crack, K_{Ic}, and blunt notch, K_B are presented as a function of testing speed. It is seen from Table II that between CHS of 0.5–50 mm min^{-1}, one obtains a (consistent) K_{Ic} around 5 MPa m$^{1/2}$. But at CHS of 500 and 1000 mm min^{-1}, the K_{Ic} is reduced to about 4 MPa m$^{1/2}$. One explanation for this difference in K_{Ic} would be in the increased yield strength of the polymer at higher CHS (Fig. 2). It should be noted that for sharp-crack specimens, the load–displacement traces at the lower speeds showed some degree of non-linearity, compared to specimens tested at higher speed (Fig. 8). The blunt notch specimens, as can be seen also in Fig. 8, showed non-linearity at all speeds. K_{Ic} and K_B were calculated from fracture loads. Hashemi and Williams [5] reported K_{Ic} of approximately 4 MPa m$^{1/2}$ for polyacetal at room temperature, while K_{Ic} of 2.8–3.6 MPa m$^{1/2}$ have been reported from catastrophic failure data in fatigue-crack propagation experiments [3, 4]. On the other hand, K_B values are higher and again consistent at all testing speeds (mean K_B = 6.29 with a standard deviation of 0.21).

TABLE II Fracture toughness: sharp crack, K_{Ic}, and blunt notch, K_B, at different test speeds

Test speed (mm min^{-1})	K_{Ic} MPa m$^{1/2}$	K_B (MPa m$^{1/2}$)
0.5	4.95	6.30
	4.95	
5	4.95	6.56
	4.63	
10	4.94	6.56
	4.89	
20	5.02	6.43
	4.95	
50	5.14	—
	5.02	
	4.89	
500	3.92	6.17
	3.86	
1000	4.05	6.24
	3.79	6.11
		5.98

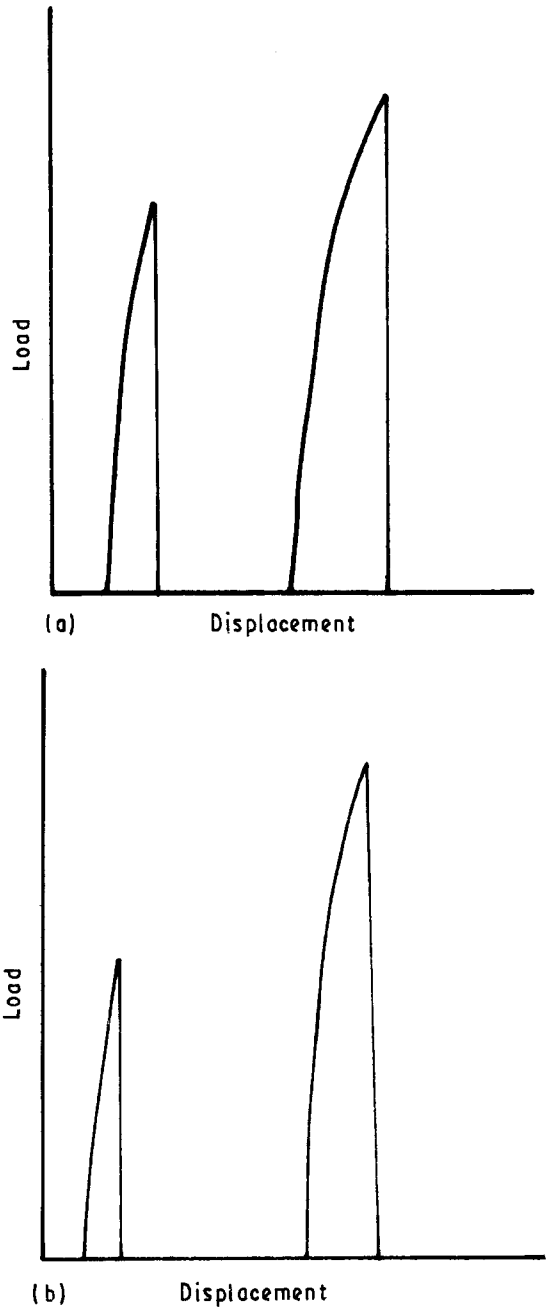

Figure 8 Load–displacement traces of SEN specimens, with (left) and without (right) a razor cut (a) at CHS 0.5 mm min^{-1}, (b) at CHS 500 mm min^{-1}. Note: The load axis is to the same scale for all specimens, whereas the displacement axes differ between (a) and (b).

Examination of fracture surfaces showed that in the blunt-notch specimens, there is a flaw-initiation region similar to that in unnotched specimens. This flaw then grows slowly followed by rapid fracture, and the whole process takes higher energy, K_B. In comparison, specimens containing razor cuts already provide an initiation site, so that the major energy-absorbing mechanisms include formation and slow advance of a natural crack, followed by rapid failure. An estimate of the plane-strain crack-tip plastic zone size, r_p, can be made by using $r_p = (1/6\pi)(K^2/\sigma_y^2)$ which gives, for example, r_p = 275 μm for a CHS of 5 mm min^{-1}, and 146 μm for a CHS of 1000 mm min^{-1}, which are usual for semi-ductile polymers [5, 12]. Fracture-surface examinations (Figs 9 and 10) show that the features in slow- and fast-growth regions are similar to those in

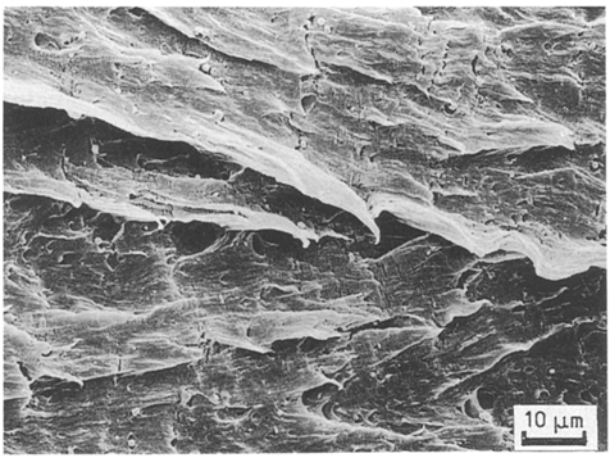

Figure 9 Fracture surface in the slow-growth region in an SEN specimen with a razor cut appears similar to that in Fig. 5. Evidence of fibrils and a large number of voids/microcracks are seen.

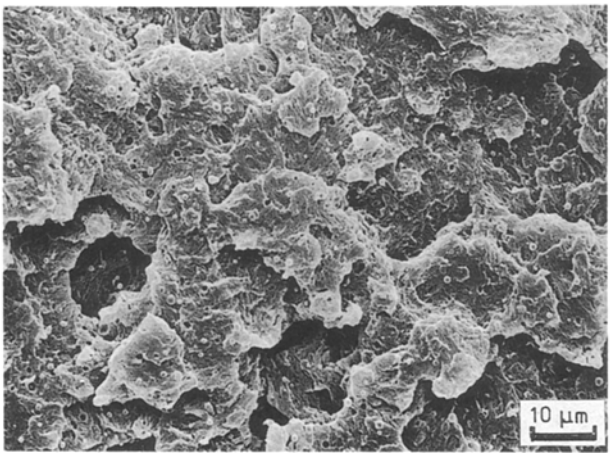

Figure 10 Fracture surface in the fast-growth region in an SEN specimen with a razor cut appears similar to that in Fig. 5. Evidence of fibrils and a large number of voids/microcracks are seen.

the case of unnotched specimens; however, there is evidence of more voiding and microcracking in Figs 9 and 10.

The size of the slow-growth region in specimens containing a razor cut is clearly influenced by the testing speed, as is evident in Fig. 11. When these are compared with those for unnotched specimens, the trend appears to be similar, and only with a difference in degree (Fig. 12).

From the slow-crack extension information of Fig. 11, if K is recalculated taking into account the amount of slow-crack extension, then one obtains an R-curve as shown in Fig. 13. Similar behaviour has been reported in the literature for some deformable polymers such as toughened epoxies [12].

4. Conclusions

1. In unnotched tensile tests, the material shows a maximum stress followed by a slow crack extension leading to rapid fracture.

2. The material behaves in a more ductile way at a slow crosshead speed such as 1 mm min^{-1}, but as the

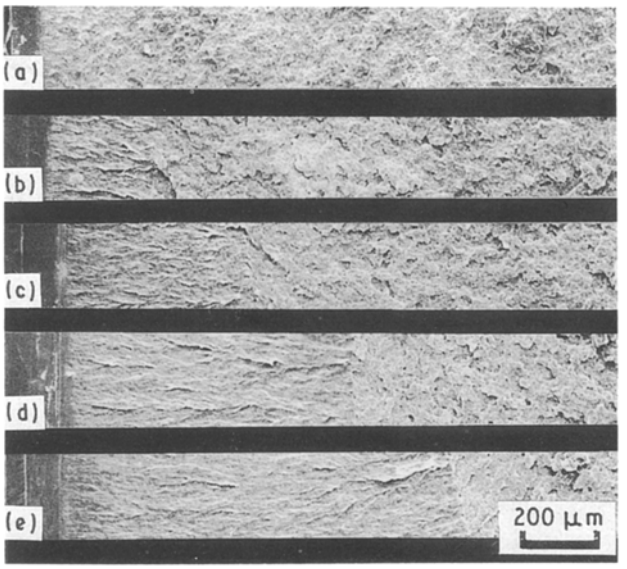

Figure 11 Comparative sizes of the slow crack-growth region in SEN specimens with a razor cut, as a function of test speed; (a) 500, (b) 50, (c) 10, (d) 5 and (e) 0.5 mm min^{-1}.

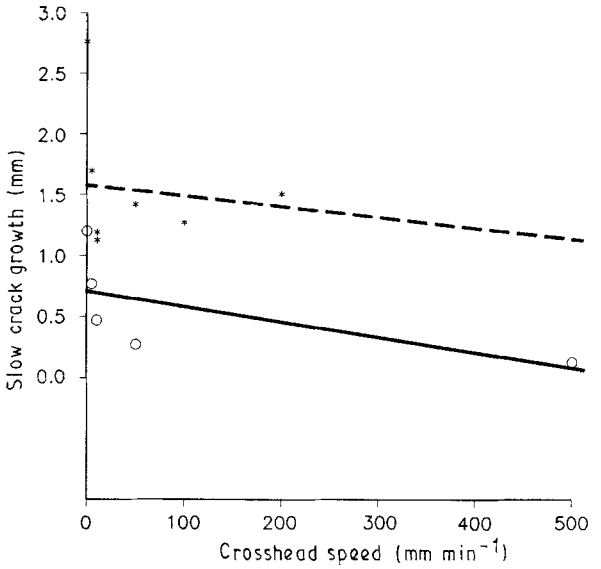

Figure 12 A comparison of the slow-growth (critical) flaw sizes in unnotched tensile specimens with those in the SEN specimens with a sharp crack: (——) notched, fracture; (– – –) unnotched, tensile.

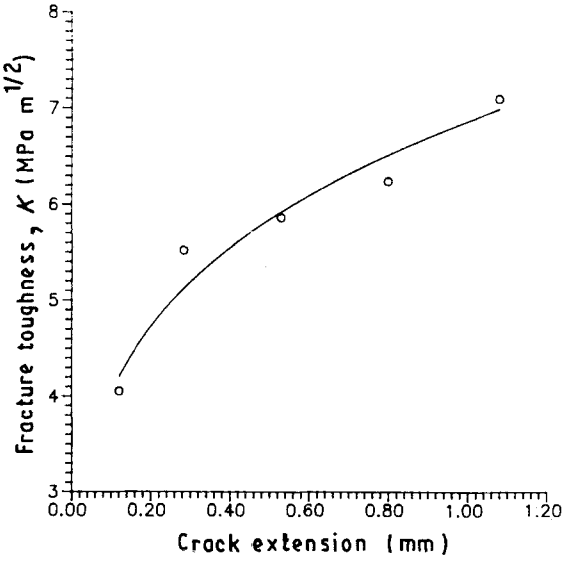

Figure 13 R-curve for the polyacetal SEN specimens.

crosshead speed is increased, the ductility quickly diminishes.

3. The yield stress (taken at the maximum load) shows a linear increase with log testing speed.

4. Failure of the unnotched specimens involves initiation of a flaw, internal or on the surface, which then grows slowly internally, until it reaches a critical size when rapid fracture sets in, and the size of the critical flaw decreases with increasing test speed. In the slow crack-growth region, failure appears to be by a void-growth mechanism, lamellar texture changing to a fibrillar one. In the fast-fracture region, the lamellar texture of the spherulites appears to be retained, however, with small voids formed in the lamellar stack.

5. In SEN specimens containing a razor cut, the fracture toughness remains constant at approximately 5 MPa $m^{1/2}$ for a CHS between 0.5 and 50 mm min^{-1}. However, at a CHS of 500 and 1000 mm min^{-1}, there is about 20% drop in the fracture toughness. The plane-strain plastic zone size accordingly reduces at higher speeds. On the other hand, blunt-notch fracture toughness appears to be unaffected by test speed and is approximately 6.3 MPa $m^{1/2}$. In these materials, the extra amount of energy is apparently utilized in initiating a flaw within the material, which subsequently grows.

6. In the SEN specimens with a razor cut, the slow crack-growth zone size increases with decreasing crack speed. The data have been utilized to construct an *R*-curve.

Acknowledgements

The authors thank Dr Brian Ennis for the DSC analysis of the polyacetal material. This work was presented at the 19th Australian Polymer Symposium, Perth, Western Australia, 2–5 February 1992.

References

1. R. CONNOLLY, R. GAUVIN and J. P. CHALIFOUX, *Polym. Engng Sci.* **25** (1985) 549.
2. F. C. CHANG and M. Y. YANG, *ibid.* **30** (1990) 543.
3. P. E. BERTZ, R. W. HERTZBERG and J. A. MANSON, *J. Appl. Polym. Sci.* **27** (1982) 1707.
4. R. W. HERTZBERG, M. D. SKIBO and J. A. MANSON, *J. Mater. Sci.* **13** (1978) 1038.
5. S. HASHEMI and J. G. WILLIAMS, *ibid.* **20** (1985) 4202.
6. E. A. FLEXMAN, D. D. HUANG and H. L. SNYDER, *Polym. Prepr.* **29** (1988) 189.
7. W. F. BROWN and J. E. SRAWLEY, ASTM Special Technical Publication **410** (1966) 1.
8. B. W. CHERRY and P. L. McGUINLEY, *Appl. Polym. Symp.* **17** (1971) 59.
9. S. BANDYOPADHYAY and H. R. BROWN, *J. Polym. Sci. Polym. Phys. Ed.* **19** (1981) 749.
10. S. BANDYOPADHYAY and H. R. BROWN, *Polymer* **22** (1981) 245.
11 W. Y. CHIANG and M. S. LO, *J. Appl. Polym. Sci.* **34** (1987) 1997.
12. S. BANDYOPADHYAY, *Mater. Sci. Engng A* **125** (1990) 157.

Received 29 January
and accepted 20 November 1992